

## EFFECT OF SQUEALER TIP ON ROTOR HEAT TRANSFER AND EFFICIENCY

**A. A. Ameri**

AYT Corporation, Brook Park, Ohio

**E. Steinthorsson**

Institute for Computational Mechanics in Propulsion (ICOMP)  
NASA Lewis Research Center

**David L. Rigby**

NYMA, Inc. NASA Lewis Group

### ABSTRACT

Calculations were performed to simulate the tip flow and heat transfer on the GE-E<sup>3</sup> first stage turbine, which represents a modern gas turbine blade geometry. Cases considered were a smooth tip, 2% recess, and 3% recess. In addition a two-dimensional cavity problem was calculated. Good agreement with experimental results was obtained for the cavity calculations, demonstrating that the  $k-\omega$  turbulence model used is capable of representing flows of the present type. In the rotor calculations, two dominant flow structures were shown to exist within the recess. Also areas of large heat transfer rate were identified on the blade tip and the mechanisms of heat transfer enhancement were discussed. No significant difference in adiabatic efficiency was observed for the three tip treatments investigated.

### INTRODUCTION

The tips of turbine blades in gas turbines experience large thermal loads which can lead to tip burnout. The large thermal load on blade tips is due to hot gases flowing through the gap between the blade tip and the shroud. The flow accelerates due to pressure difference between the pressure and suction sides, causing thin boundary layers and high heat transfer rates. The flow across the tip is also undesirable from the perspective of efficiency since it increases the losses in the flow.

A common strategy to reduce the flow on the tip is to use a recessed tip, also known as a squealer tip. By using a squealer tip, the tip gap can be made smaller without the unacceptable risk of catastrophic failure should the tip rub against the shroud in the course of turbine operation. The smaller gap reduces the flow rate through the tip clearance, which leads to smaller losses and lower heat transfer. It is believed that the tip recess also acts to increase the resistance to the flow (Metzger et al., 1989).

In order to study the effects of a squealer tip geometry on heat transfer and losses, Metzger et al. (1989), and Chyu et al. (1989) performed experiments using cavities of varying depth to width and gap to width ratios. As a result of these experiments Metzger et al. made a number of important conclusions. In particular, they concluded that for a given pressure difference across the gap there is an optimum value of depth to width ratio beyond which no further flow reduction will occur. They also concluded that

although the rate of heat transfer on the cavity floor is lower than that on a flat tip, the reduction in heat transfer is offset by the high heat transfer in the redeveloping flow on the downstream gap and by the additional heat transfer area created on the side walls. Thus, they recommended that shallow cavities are preferred if overall heat transfer reduction on the cavity wall is the goal.

The experimental studies cited above provide insight into the nature of the flow field around the squealer tip. However, actual turbine blades differ greatly from the idealized experimental setup. The flow in the blade tip and gap are highly three-dimensional. The relevant parameters, namely, depth to width and clearance gap to width ratios of the recess vary widely along the gap. The pressure difference across the tip also varies widely along the blade. Thus it is unlikely that a simple model will provide designer of a turbine blade with the information needed to understand the flow in the tip region. At the present time neither experimental data nor numerical simulations are available in open literature that shed light on the details of the flow and heat transfer on a squealer tip flow. Also, with the exception of the heat transfer data of Yang and Diller (1995) which was taken at a single point on the cavity floor of a rotor blade, there are no data available on heat transfer on squealer tips. In this paper we conduct a numerical study of heat transfer on a squealer tip of a generic modern gas turbine blade. This numerical simulation also allows insight into the nature of the flow within the cavity and its effects on efficiency. The blade chosen for this study is the General Electric E<sup>3</sup> design detailed in two NASA reports (Halila et al., 1982 and Timko 1982). The numerical simulations of the heat transfer within the simplified squealer tip model used by Metzger et al. (1989) are first performed with a view to demonstrate the ability of the numerical model to accurately predict the flow and heat transfer as well as to forewarn us as to the possible limitations of the analysis.

In the section to follow we will give a brief description of the numerical method used in the simulations, the turbulence model and the numerical boundary conditions. Afterwards we will present the results of heat transfer predictions and

comparison with experimental data on the walls and rim of transverse grooves used in the experiments cited above to simulate the squealer tip. We will subsequently show the heat transfer results obtained for the GE-E<sup>3</sup> turbine blade for a flat tip and two recessed tip cases and discuss the results. Finally we will present the calculation of efficiency and close by presenting a summary and the conclusions.

## COMPUTATIONAL METHOD

The simulations performed in this study were done using a multi-block computer code called TRAF3D.MB (Steinthorsson et al. 1993). This code is a general purpose flow solver designed for simulations of flows in complicated geometries. The code is based on TRAF3D, an efficient computer code designed for simulations of steady flows in turbine cascades (Arnone et al. 1994). The TRAF3D.MB code solves the full compressible Navier-Stokes equations. It uses the finite volume method to discretize the equations. The code uses central differencing together with artificial dissipation to discretize the convective terms. The overall accuracy of the code is second order. The TRAF3D.MB code was described in detail by Steinthorsson et al. (1993). The present version of the code which employs a two-equation model has been used in connection with an internal flow calculation of heat transfer as described by Rigby et al. (1996)

### Turbulence and Transition Models

Algebraic model of Baldwin and Lomax (1978) has been quite successful in predicting the rate of heat transfer to turbine blades. Combining this turbulence model with other models simulating laminar-turbulent transition and models simulating leading edge heat transfer enhancement have been shown to produce accurate results (Ameri and Arnone 1996, Boyle(1991). When using a multiblock approach in connection with complex geometries involving many no-slip surfaces, it is advantageous to use a turbulence model that does not require the computation of the dimensionless distance to the wall ( $y^+$ ) as is done in Baldwin-Lomax zero equation model and many two-equation models. Therefore, for the present computations, it was decided to use the  $k-\omega$  turbulence model developed by Wilcox (1994a,1994b) with subsequent modifications by Menter (1993). The model integrates to the walls. Chima (1996) incorporated the latter model in a Navier-Stokes solver and presented results of its application to turbomachinery flows and heat transfer. Below we present the equations describing the turbulence in tensor notation.

$$(\rho s_i)_{,t} + (\rho s_i u_j + q_{ij})_{,j} = \frac{1}{\rho}(P - D) \quad (1)$$

$$q_{i,j} = -\left(\mu + \frac{\mu_t}{\sigma}\right)s_{i,j} \quad i=1,2 \quad (2)$$

where  $s_1=k$  and  $s_2=\omega$  also  $\mu_t=\alpha^* \frac{\rho k}{\omega}$ . The production source terms,  $P$ , of equation (1) are defined as:

$$\frac{P}{\rho} = \begin{bmatrix} \frac{Re^{-1}}{\rho} \mu_t \Omega^2 - u_{i,i} \\ \alpha \left[ \alpha^* \Omega^2 - \frac{2}{3} \omega u_{i,i} \right] \end{bmatrix} \quad (3)$$

where  $\Omega$  is the magnitude of vorticity. The destruction terms,  $D$ , are given by

$$\frac{D}{\rho} = \begin{bmatrix} \beta^* \omega k \\ \beta \omega^2 \end{bmatrix} \quad (4)$$

The coefficients appearing in the model are as follows:  
 $\sigma=2.0$ ,  $\beta=3/40$ ,  $\beta^*=0.09F_\beta$ ,  $\alpha=(5/9)(F_\alpha/F_\mu)$ , and  $\alpha^*=F_\mu$ ,  
 where

$$F_\beta = \frac{5/18 + (Re_T/R_\beta)^4}{1 + (Re_T/R_\beta)^4} \quad (5)$$

$$F_\alpha = \frac{\alpha_0 + (Re_T/R_\omega)}{1 + (Re_T/R_\omega)} \quad (6)$$

$$F_\mu = \frac{\alpha_0^* + (Re_T/R_\beta)}{1 + (Re_T/R_\beta)} \quad (7)$$

$$Re_T = \frac{\rho k}{\mu \omega} \quad (8)$$

$\alpha_0=0.1$ ,  $\alpha_0^*=0.025$ ,  $R_\beta=8$ ,  $R_\omega=2.7$  and  $R_k=6$ .

The turbulent thermal diffusivity is computed from:

$$\alpha_t = \frac{\mu_t}{\rho Pr_t} \quad (9)$$

where  $\rho$  is density. A constant value of 0.9 is used for turbulent Prandtl number  $Pr_t$ .

### Boundary Conditions

The types of boundary conditions encountered are as follows:

1) Inlet: The inlet boundary condition for axially subsonic flows is treated by specifying the inlet total temperature and inlet total pressure as well as the inlet angle profiles. The outgoing Riemann invariant is extrapolated to the inlet from within. The total temperature and total pressure profiles are determined to match the law of the wall for the specified hydrodynamic and thermal boundary layer thicknesses on the hub and/or the shroud. For the turbulence quantities for the blade row, an inlet turbulence intensity of 8% and a length scale of 10% of axial chord is used. These values are estimated and believed to be representative of the conditions existing at the inlet of the blade row.

2) Exit: At the exit boundary, for the subsonic axial flow, the pressure is specified and all the other conditions (including the turbulence quantities) are extrapolated from within. The pressure at the exit plane for the turbine blade considered here is computed



herein are spatially converged. Note that in the computations, the grid in the exit region was extended to allow complete flow attachment very near the rim before exiting the computational domain.

Figure 3 presents the rate of heat transfer as computed and measured for the deeper cavity. The abscissa is the string distance measured along the rim and walls of the cavity, starting from  $x=0$ ,  $y=4$ . The ordinate is the Nusselt number defined as:

$$Nu = \frac{hc}{k} \quad (12)$$

In Eqn. 11,  $h$  is the heat transfer coefficient based on the inlet temperature,  $c$  is the inlet gap height and  $k$  is thermal conductivity of the bulk inlet flow. The figure shows generally good agreement between the experimental results and the analysis. However a large rise in heat transfer is predicted on the upper portion of the downstream side wall. A rise in the rate of heat transfer in that region is expected to exist due to flow stagnation. The data however do not indicate as large a rise as predicted by the analysis.

In Fig. 4 the comparison between analysis and experimental data for the shallow cavity is presented. The experimental data were taken on the rim and the bottom of the cavity but not on the side walls. Again it is observed that the agreement in general is good.

Finally, in Fig. 5 the measured pressure loss coefficients defined as:

$$f = (\Delta p C) / (2L\rho V^2) \quad (13)$$

are plotted as a function of cavity depth ratio for three families of gap clearance ratios. In the above definition,  $L$  is the gap length in flow direction and  $\rho$  and  $V$  are the bulk density and velocity of the inlet flow and  $\Delta p$  is the pressure difference across the gap. The calculated values of the pressure loss coefficient for the two cases considered here are superimposed on this plot using open symbols. The agreement is very good.

The two computed cases of flow in a cavity, demonstrate the capability of the present turbulence model to produce results of reasonable accuracy for this particular type of flow. Although this flow is essentially two-dimensional while the flow on a blade tip is three-dimensional, these results lend credence to the predictions presented in the following section. The turbulence model has been shown to perform quite well for flow and heat transfer predictions on turbine blades as was demonstrated by Chima(1996).

## Blade Tip

**Geometry and the grid.** The geometry of the GE-E<sup>3</sup> blade with the simulated squealer tip is shown in Fig. 6a. The blades have a constant chord length of 2.87 cm and an aspect ratio of 1.39. A squealer tip thickness of 0.030 in. (0.77 mm) was chosen for this study. Three geometrical cases were considered, a flat tip, and two typical tip recesses of 2% and a 3%. The tip gap clearance was 1% for all the three cases. Figures 6b and 6c show the grid on the blade, the hub and the tip surfaces. Note that every other grid line has been eliminated for clarity. The grid topology is essentially the same as given in Ameri and Steinhilber (1996) with the exception of the grid in the tip. For the present geometry, the tip grid is constructed using two blocks. One block covers the entire tip clearance excluding the cavity while the second block covers the space within the cavity. Grid is refined close to all no-slip surfaces such that the distance of the cell centers adjacent to solid walls, measured in wall units ( $y^+$ ), is close to unity. This aspect of the grid construction is

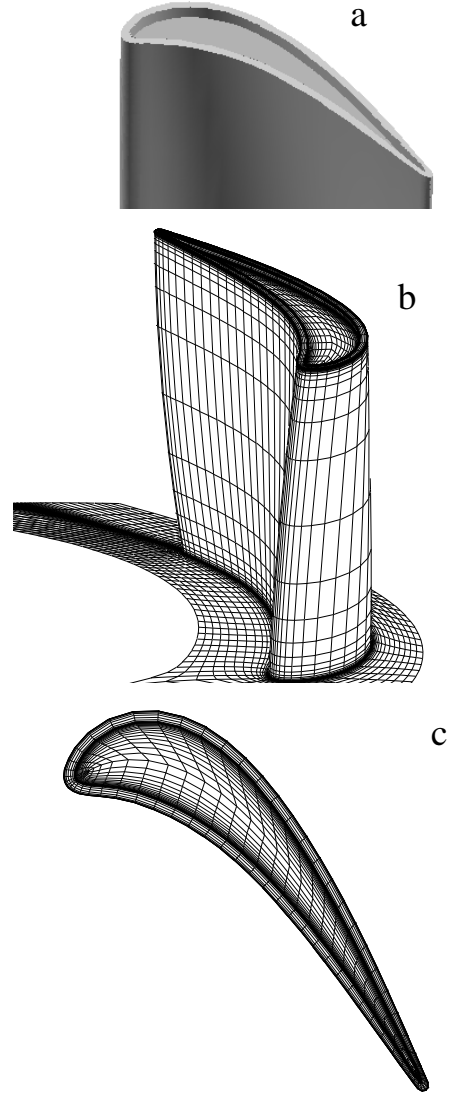


**Fig. 6** Geometry and grid distribution for the E<sup>3</sup> blade. Alternate grid lines are eliminated for clarity.

crucial to both the solution accuracy and to convergence. The dimension of the C grid covering the blade from hub to shroud is 193x49x99. In the tip clearance the grid dimension is 129x57x33. In the cavity there are 129x 33x 41 grid points for both the 2% and the 3% cases. The flat tip case was run with the same grid in the tip as the recessed cases(129x 57x 33) to allow direct comparison of heat transfer devoid of resolution differences. A single block of 9x9x99 grid points covers the entire inlet upstream of the blade.

**Flowfield.** The conditions used for the numerical simulations are the same as experimental conditions of the warm rig used by Timko (1982) for the GE-E<sup>3</sup> turbine and are as listed in Table 1. The inlet angle variation is taken

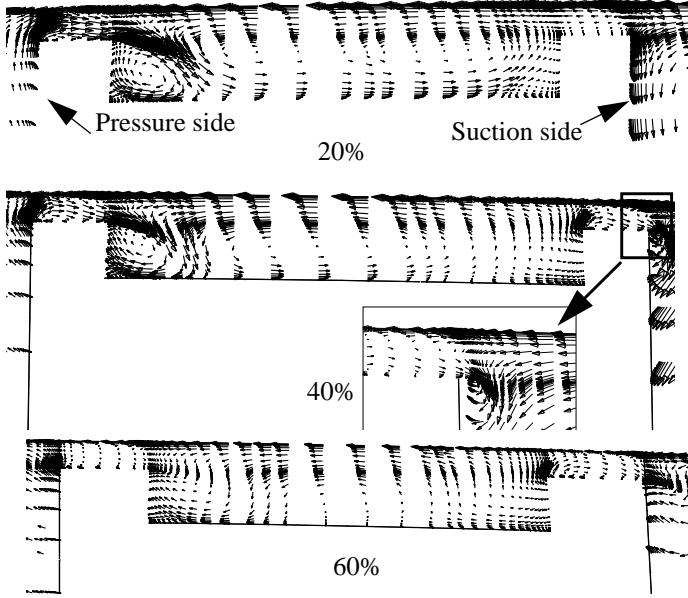


**Fig. 7** View of the velocity vectors in and around the tip at various axial locations for the case of 3% recess.

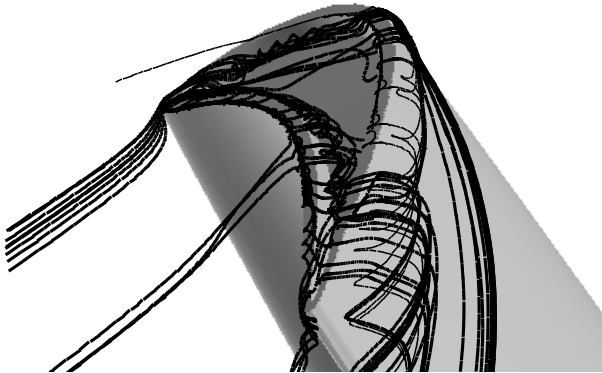


**Fig. 8** Streamlines showing the blade tip flow patterns.

**TABLE 1. Run conditions**

Absolute pressure Ratio across the Blade Row	0.44
Absolute inlet angle	69° Hub 74.5° Mid Span 78.5° Shroud
Rotation Rate	8450 RPM
$T_w/T_t$	0.7

from measurements but the wall to total temperature ratio was set at a typical value.

In Figure 7 plots of computed velocity vectors in the tip region projected on planes normal to the machine axis for various axial locations are shown. The flow is shown in the rotating blade frame

of reference, hence the nonzero velocity on the shroud. The tip flow is highly three-dimensional. The variation in flow patterns in the tip clearance is apparent from examining the vector plots. For the 20% to 60% axial distance the plots show a complex system of vortices in the tip clearance. Figure 8 shows the streamline patterns in the tip. In that figure at least two distinct vortices can be discerned to exist within the cavity. One vortex is a separation vortex, generated as the incoming flow separates off the inner edge of the pressure side rim. This vortex hugs the pressure side, sidewall and “spills” out of the cavity near the trailing edge of the blade. The second vortex which is apparently also a separation vortex, runs from the stagnation region to the suction side of the blade. These vortices are generated in addition to the separation vortex along the pressure side rim, suction side rim and the blade suction side tip flow vortex.

This vortex system apparently offers additional blockage to the flow through the gap. The flow rate through the tip gap for the flat tip case was calculated to be 1.98% of the mass flow through the blade row. The 2% and 3% recessed blades had leakage mass flow rates of 1.8% and 1.7% of the total mass flow rate equivalent to 90% and 86% of that of the flat tip case.

**Heat Transfer** The rate of heat transfer is presented in terms of Stanton number defined as:

$$St = \frac{h}{\rho_{ref} V_{ref} C_p} \quad (14)$$

where  $h$  is the heat transfer coefficient based on the absolute inlet total temperature. The reference velocity is the average relative velocity at a location 20% of the axial chord upstream of the blade. The reference temperature is the average absolute total temperature and the reference density is the average density at that location. (The inlet relative total temperature at the midspan is 0.879 times the absolute inlet total temperature.)

Heat transfer rates on the blade surface at three spanwise locations are given in Fig. 9. This figure serves as a guide as to the magnitude of the tip heat transfer as compared to the blade surface heat transfer.

The heat transfer results on the tip of the blade are given in Fig. 10a-c. Fig. 10a shows the Stanton number distribution on the flat tip surface. The patterns of heat transfer contours on the blade tip are as expected and have been seen before in connection with our previous studies (Ameri & Steinthorsson 1995 and 1996). Those patterns include, sharp entrance effect on the pressure side of the tip surface where the rate of heat transfer reaches a maximum due to flow reattachment; the ensuing drop in heat transfer downstream of that location; a large rate of heat transfer around the corner from the blade stagnation point and the large increase in heat transfer on the suction side of the blade (near the crown). The average level of heat transfer on the flat tip is similar in magnitude to the heat transfer rate on the blade leading edge. For the two recessed cases the heat transfer distribution is shown using one figure which shows the heat transfer on the bottom of the cavity and the rim surface of the squealer tip and a separate Fig. 11 to show the heat transfer on the side-wall of the recess. Fig. 10b and c show the heat transfer on the surfaces of the 2% and 3% cavity, respectively. It is observed that the rate of heat transfer on the bottom of the cavity reaches higher values than is seen on the flat tip. On the rim the rate of heat transfer on the pressure side is comparable to the flat case but is somewhat higher

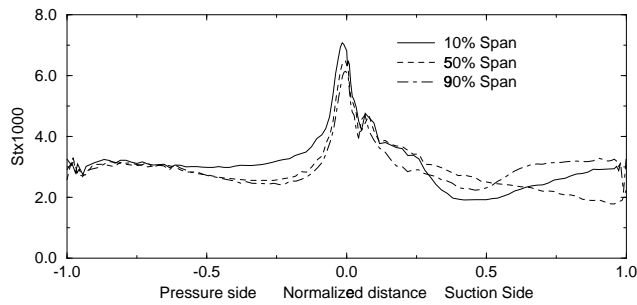


**Fig. 9** Surface heat transfer at 10%, 50% and 90% span on the flat tipped blade.

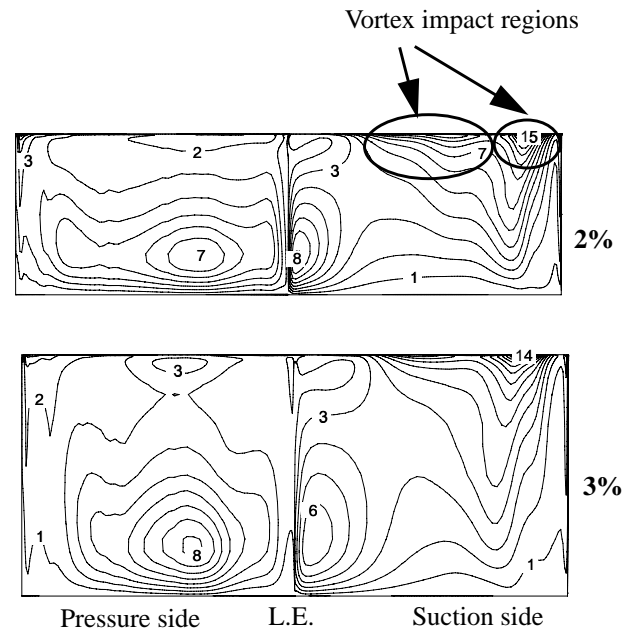


**Fig. 11** Heat transfer distribution on the side wall of the cavity as unwrapped about the minimum x location in terms of  $1000 \times St$ .

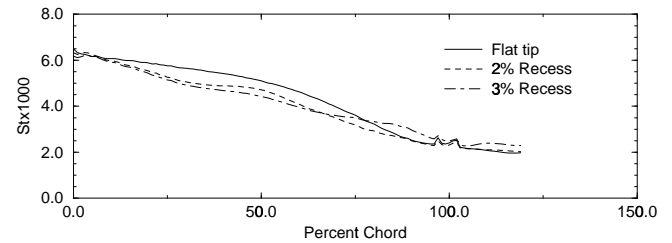


**Fig. 12** Tangentially averaged shroud heat transfer

on the suction side. The large rate of heat transfer on the bottom of the cavity is due to flow impingement containing hot gas. This impingement can best be seen in Fig. 7 for the 20% axial distance.

It is worth mentioning that in both the experimental investigations cited above, the rate of heat transfer on the bottom of the cavity was always observed to be less than that on the rim. However, in their numerical calculations, Chyu et al. (1987) do show instances where the bottom of the cavity has substantially higher heat transfer coefficient compared to the rims.

Squealer side wall heat transfer is presented in Fig. 11. The inside wall surface is unwrapped around the minimum axial location. The ordinate is exaggerated for clarity. The abscissa is the axial chord distance. Areas of large heat transfer rates are generated as a result of the vortical action inside the cavity. The vortical action increases due to flow acceleration and stretching of these vortices. The highest rate of heat transfer is observed to exist near the trailing edge of the blade on the suction side wall. The cause of this increase was found to be the impact of the vortex spillage with the side wall. As such this rise in heat transfer, although present may be exaggerated as was discussed in connection with the two-dimensional cavity.

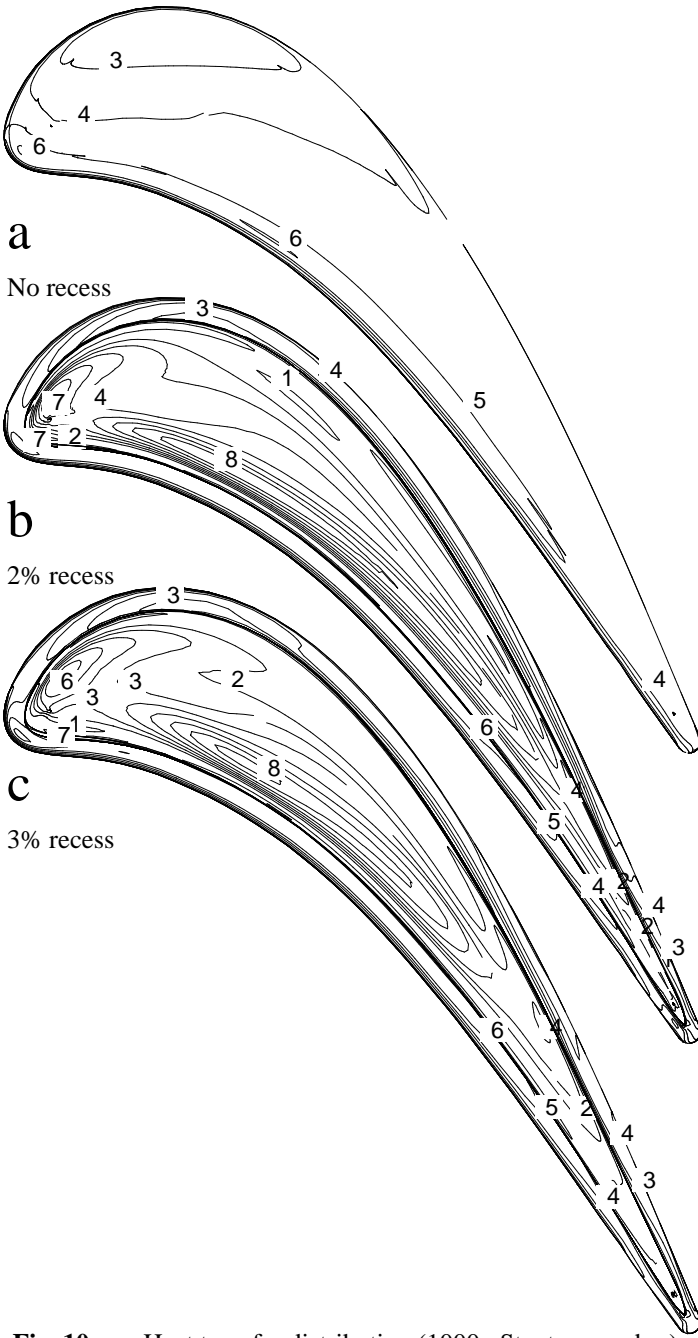


**Fig. 10a-c** Heat transfer distribution ( $1000 \times$  Stanton number) on the cavity floor and rim for no recess as well as 2 and 3% tip recess.

The shroud heat transfer is presented in Fig. 12. As can be seen from this figure the rate of heat transfer on the shroud is higher for the flat tip case as compared to the two recessed cases.

Finally the total tip heat transfer for the three cases was compared. It was found that the 2% and 3% recess cases, had an increase of 80% and 90% respectively in total heat addition to the tip compared to the flat tip case of the same tip clearance.

### Efficiency

As a by-product of our heat transfer computations, it is possible to compute the efficiency and the possible effect of recess on efficiency. The expression for the adiabatic efficiency is

$$\eta = \frac{T'_{in} - T'_{ex}}{T'_{in} \left[ 1 - \left( \frac{p'_{ex}}{p'_{in}} \right)^{(\gamma-1)/\gamma} \right]} \quad (15)$$

In Eqn. 14 the primes signify relative total values, subscript *in* and *ex*, signify inlet and exit mass averaged values and  $\gamma$  is the specific heat ratio. The calculated efficiency is based on the assumption of an ideal stator upstream and the average inlet values are computed at 20% axial chord upstream of the rotor. The exit values are computed at 50% axial chord downstream of the rotor. Because the blade surface temperature was set at a constant temperature of 0.7xthe inlet total temperature, in order to recover adiabatic conditions, the gas total temperature at the exit was modified to reflect the loss of energy through heat transfer. Failure to do so leads to an error of 5 points in the efficiency for the present computations. The change in mass averaged normalized total temperature at the exit of the blade row can be computed as follows:

$$\Delta T'_{ex} = \frac{\sum \int_A (\mu \partial T / \partial n|_w) dA}{\dot{m} \text{RePr}} \quad (16)$$

In the above equation  $\mu$  is dimensionless viscosity and *n* is the normalized distance to the wall  $\dot{m}$  is the normalized mass flow rate through the blade passage and *A* is the surface area. The integration is performed over all of the heat transfer surfaces. The mass averaged value of the exit total temperature is thus computed as:

$$T'_{ex} = T'_{unmodified} + \Delta T'_{ex} \quad (17)$$

The efficiency for the row of blades was computed to be 91.3%, 91.4% and 91.4% for the 0%, 2% and 3% recess cases, in spite of the fact that there was a 10 to 14% reduction in gap flow.

### SUMMARY AND CONCLUSIONS

In this paper, results are presented from three-dimensional simulations of flow and heat transfer over a turbine blade with a squealer tip. The simulations were carried out using a second order accurate finite volume scheme on a multi-block grid system containing 1.2 million grid points. Effects of turbulence on the flow field were modeled using a k- $\omega$  two-equation turbulence model. The ability of the turbulence model to predict the heat transfer in flows of the type considered here was verified by simulating the flow in a two-dimensional model of squealer tips for which experimental data is available. For the three-dimensional case an actual modern gas turbine geometry, namely the GE-E<sup>3</sup> first stage turbine blade was used. Two

dominant vortical structures were identified to exist in the recess region. The heat transfer rate on the recess surfaces were found to be strongly affected by these flow structures. Especially high heat transfer rates were observed where the vortices exit the recess region. No significant effect due to the recessed tip on efficiency was detected although the mass flow rate through the tip gap was found to be smaller by as much as 14% for the squealer tip as compared to flat tip of the same clearance height.

### ACKNOWLEDGEMENT

The authors wish to express their gratitude to Dr. Raymond Gaugler, Chief of the Turbine Branch, as well as to Dr. Louis Povinelli, Chief of the Turbomachinery and Propulsion Systems Division of NASA Lewis Research Center and Director of ICOMP for their support and encouragement of this work. Thanks are also due to Mr. Robert Boyle for his suggestions and his guidance. The computations were performed on the CRAY-C90 of NAS at NASA Ames Research Center.

### REFERENCES

- Ameri, Ali A., and Steinhorrson, E., 1995, "Prediction of Unshrouded Rotor Blade Tip Heat Transfer," ASME 95-GT-142.
- Ameri, Ali A., Arnone, A., 1996, "Transition Modeling Effects on Turbine Rotor Blade Heat Transfer Predictions," *J. of Turbomachinery*, Vol. 118, pp. 307-313.
- Ameri, Ali A., and Steinhorrson, E., 1996, "Analysis of Gas Turbine Rotor Blade Tip and Shroud Heat Transfer," IGTI 96-GT-189.
- Arnone, A., Liou, M. S., and Povinelli, L. A., 1994, "Viscous Analysis of Three-Dimensional Rotor Flow Using a Multigrid Method," *J. of Turbomachinery*, Vol. 116, pp. 435-445.
- Baldwin, B. S. and Lomax, H., 1978, "Thin Layer Approximation and Algebraic Model for Separated Turbulent Flows," AIAA paper 78-0257.
- Boyle, R. J., 1991, "Navier-Stokes Analysis of Turbine Blade Heat Transfer," *J. of Turbomachinery*, Vol. 113, pp. 392-403.
- Chima, R. V. 1996, "A k- $\omega$  Turbulence Model for Quasi-Three-Dimensional Turbomachinery Flows," AIAA paper 96-0248
- Chyu, M.K., Moon, H.K. and Metzger, D.E., 1989, "Heat Transfer in the Tip Region of Grooved Turbine Blades," *J. of Turbomachinery*, Vol. 111, pp. 131-138
- Chyu, M.K., Metzger, D.E. and Hwan, C. L., 1987, "Heat Transfer in Shrouded Rectangular Cavities," *J. of Thermophysics*, Vol. 1, No.3, July 1987, pp 247-252.
- Halila, E. E. and Lenahan, D. T., and Thomas, L. L., 1982, "Energy Efficient Engine, High Pressure Turbine Test Hardware Detailed Design Report," NASA CR-167955.
- Menter, Florian R., 1993, "Zonal Two-Equation k- $\omega$  Turbulence Models for Aerodynamic Flows," AIAA-93-2906.
- Metzger, D. E., Bunker, R. S. and Chyu, M. K., 1989, "Cavity Heat Transfer on a Transverse Grooved Wall in a Narrow Channel," *J. of Heat Transfer*, Vol. 111, pp. 73-79.
- Rigby David, L., Ameri Ali, A. and Steinhorrson E., 1996, "Internal Passage Heat Transfer Prediction Using Multiblock Grids and k- $\omega$  Turbulence Model," IGTI paper 96-GT-188.
- Steinhorrson, E., Liou, M. S., and Povinelli, L.A., 1993, "Development of an Explicit Multiblock/Multigrid Flow Solver for Viscous Flows in Complex Geometries," AIAA-93-2380.

Timko, L.P., 1982, "Energy Efficient Engine High Pressure Turbine Component Test Performance Report," NASA CR-168289.

Wilcox, D. C., 1994a, "Turbulence Modeling for CFD," DCW industries, Inc. La Canda, CA.

Wilcox, D. C., 1994b, "Simulation of Transition with a Two-Equation Turbulence Model," AIAA Journal, Vol. 32, No.2, pp.247-255.

Yang, Timothy, T. and Diller, Thomas, E., "Heat Transfer and Flow for a Grooved Turbine Blade Tip in a Transonic Cascade," ASME paper No. 95-WA/HT-29.